RSC Advances

ROYAL SOCIETY OF CHEMISTRY

www.rsc.org/advances

Journal Name

ARTICLE

Versatility and robustness of ZnO:Cs electron transporting layer for printable organic solar cells

Received 00th January 20xx,
Accepted 00th January 20xx

DOI: 10.1039/x0xx00000x

www.rsc.org/

Lijian Zuo, Shuhua Zhang, Shuai Dai, Hongzheng Chen*

In this work, the Cs doped sol-gel ZnO film (ZnO:Cs) as efficient and robust electron transporting layer (ETL) in versatile systems of organic solar cells (OSCs) is developed, which can be simply formulated by blending the Cs_2CO_3 with the $Zn(Ac)_2$ precursor in solutions. The Cs doping significantly increased the ZnO film conductivity and lowered its work function, as unveiled by the conductive atomic force microscope and the ultra-violet photoelectron spectroscopy. Decent device performance enhancements of OSCs with versatile photovoltaic materials, e.g. P3HT:PC_{61}BM, P3HT:ICBA, and PTB7:PC_{71}BM, were observed with the doped ZnO:Cs as the ETL compared with the pristine ZnO ETL. The enhanced device performance was also found in the tandem solar cells. Moreover, the device performance shows little drop with the thickness of the doped ZnO:Cs ETL ranging from 40 to 520 nm, indicating the less thickness dependence for the doped ZnO:Cs ETL. The current work verifies the potential of the Cs doped ZnO as a high performance ETL material for printable OSCs.

Introduction

The simple **M**etal/**S**emiconductor/**M**etal (MSM) structured photovoltaic devices[1-3] are emerging as one promising technique for solar energy conversion, e.g. organic solar cells (OSC)[4, 5]. The inherent merits of OSC include low cost, flexible, light-weight, and compatible with the Roll to Roll (R2R) processing[6, 7], which endow it the strong competitiveness for future commercialization[8, 9]. In this structure, the active layer functions as both light absorbing and charge transporting layer[10]. Due to the bipolar charge transporting property of these sandwiched active layers, the device polarity is determined mainly by electrodes, e.g. the electronic structure or the energy level alignment at the electrode interfaces. To realize high device performance, efficient and selective transporting of only one charge species is required to reduce the charge recombination[11-16]. As a result, the cathode work function comparable with the Lowest Unoccupied Molecular Orbit (LUMO) is desired to form Ohmic contact for the electron extraction, and vice verse for the anode with work function comparable to the Highest Occupied Molecular Orbit (HOMO) for the hole extraction. Since the intrinsic work function of the electrode is limited by its own nature, modification of the electrode is essentially important to achieve the optimal interface contact and the high device performance[17-21].

The commercially available poly(3,4-ethylenedioxythiophene):poly(styrene sulfonate) (PEDOT:PSS) is a versatile anode modification layer due to the doping induced high conductivity and high work function[22]. However, the cathode interfacial modification materials or the electron transporting layer (ETL) with versatility are lacked. A general rule for designing the optimal ETL is to lower the work function and increase the conductivity of ETL, as unveiled previously[15]. Recently, a variety of candidates for cathode modification were reported, e.g. bathocuproine (BCP)[23, 24], Aluminum 8-hydroxyquinolinate (AlQ_3)[25], LiF[26], ZnO[27], TiO_2[28], poly electrolytes[8], etc. Most of them could lower the electrode work function to efficiently extract electrons while suppress the holes, with the mechanisms of doping effect[29, 30], intrinsic low work function[31-33] or the formation of favorable dipole moments[34, 35]. Although these ETLs could promise the OSC with enhanced device performance, the film thickness was critically limited within tens of nanometers. Generally, thicker films would block the charge extraction and ruin the device performance due to the low conductivity of these ETLs. Notably, the thin films (several tens of nm) could hardly make a full coverage on the rough electrode surfaces, which might lead to punctures and cause charge recombination. And the ultra-thin and homogeneous film on large area substrates is especially difficult to form on the rough R2R processing[36]. Therefore, it is urging to develop new ETLs with high efficiency, versatility, and processing robustness for R2R integration[36, 37]. One possible strategy to resolve this problem is by doping, with which the film conductivity would increase appreciably and the work function could also be tuned to an appropriate energy level[38-42].

In this work, we demonstrated a Cs doped sol-gel ZnO film (ZnO:Cs for short) as the efficient and robust ETL for printable OSCs. Compared with the pristine ZnO ETL, the device

State Key Laboratory of Silicon Materials, MOE Key Laboratory of Macromolecular Synthesis and Functionalization, Department of Polymer Science & Engineering, Zhejiang University, Hangzhou 310027, China,
† E-mail: hzchen@zju.edu.cn

performance with the Cs doped ZnO as ETL was enhanced in OSCs with a variety of photovoltaic materials (chemical structures shown in **Figure 1a**), e.g. poly (3-hexylthiophene) (P3HT):[6,6]-phenyl-C61-butyric acid methyl ester ($PC_{61}BM$), P3HT:indene-C60 bisadduct (ICBA), and poly(benzodithiophene-alt-thienothiophene) (PTB7): [6,6]-phenyl-C71-butyric acid methyl ester ($PC_{71}BM$), in both single junction (**Figure 1b**) and tandem (**Figure 1c**) device architectures. Less thickness dependence was also found for the doped ZnO:Cs ETL, indicating its versatility and robustness as a potential ETL material for printable OSCs.

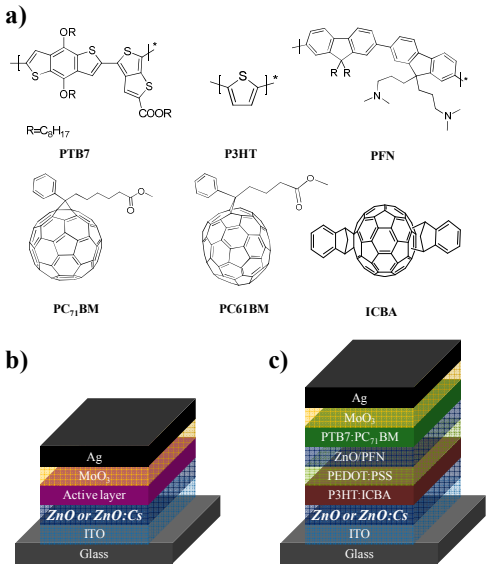

Figure 1. a) Chemical structures of the materials used in this work, **b)** Schematic device structure of the inverted single junction organic solar cells, **c)** Schematic device structure of the inverted tandem organic solar cells.

Experimental section

Materials and Equipments

All of the chemicals are purchased from Sigma Aldrich if not specified. The P3HT and PTB7 are purchased from 1-materials Corp and used as received. The $IC_{60}BA$ and $PC_{61}BM$ are purchased from Lumi. Tech. (Taiwan, China), and used as received. The UPS measurement was carried out on an integrated ultrahigh vacuum system equipped with multi-technique surface analysis system (Thermo ESCALAB 250Xi) with the He (I) (21.2 eV) UV excitation source. The atomic force microscopy (AFM) was recorded by the Nanscope IIIa multi-mode scanning probe microscope. The conducting AFM (c-AFM) was measured at contact mode with a Pt coated tip. A plastic tip holder was used for the measurement.

Device fabrication and measurement

Single junction organic photovoltaic devices

The patterned ITO/glass substrates were cleaned sequentially by detergent, acetone, isopropanol in ultrasonic bath. After blew dry by N_2 gas, the substrates were further cleaned by UV-Ozone machine. ZnO precursor solution (0.5 M $Zn(Ac)_2 \cdot 2H_2O$ in 2-methoxyethanol, with 0.5 M monoethanolamine, with or without 0.005 M Cs_2CO_3) was spun on the ITO substrate at 3000 rpm and annealed at 160 ^{o}C for 30 min to form 30-40 nm ZnO or the doped ZnO:Cs ETL. The substrates were transferred into the glove-box to deposit the BHJ layer. For P3HT:$PC_{61}BM$ layer, 30 mg/ml (P3HT:$PC_{61}BM$=1:1 wt%) o-dichlorobenzene solution is spun on the substrate to form a 120 nm film. To control the morphology of the active layer, slow growth method was adopted. The dried P3HT:$PC_{61}BM$ film was further annealed at 120 °C for 5 min to improve the crystalline properties. Finally, 10 nm MoO_3 and 100 nm Ag layers were deposited sequentially in vacuum to complete the device fabrication process. The deposition of P3HT:ICBA is the same to that of P3HT:$PC_{61}BM$, except that the modified PEDOT:PSS (m-PEDOT:PSS) instead of MoO_3 is used as HTL. The deposition of the m-PEDOT:PSS) is described elsewhere [44]. For the PTB7:$PC_{71}BM$ solar cell, 25 mg PTB7:$PC_{71}BM$ composite (PTB7:$PC_{71}BM$=1:1.5, wt%) was dissolved in 1 ml chlorobenze mixed with 3% diiodooctane by volume, and stirred over night at 70 ^{o}C for complete dissolution. Then, the solution was spin-casted onto ITO/ZnO substrates to form a film of 80 nm thickness. After that, 10 nm MoO_3 and 100 nm Ag layers were deposited sequentially.

Tandem solar cells

The fabrication of glass/ITO/ZnO or ZnO:Cs/P3HT:ICBA/m-PEDOT:PSS substrates is the same as that for the single junction device mentioned above. On the prepared substrates, the ZnO precursor solution, consisting of 20 mg/ml zinc acetylacetonate hydrate in anhydrous methanol was spin-coated onto cleaned ITO-coated glass, followed by thermal annealing in air at 90 ° C for 3 min (ca. 20 nm). Subsequently, PFN in methanol solution was deposited on ZnO layer using a spin-coating process. The same procedure for the active layer in the single junction device was used for the PTB7:$PC_{71}BM$ deposition. Finally, the substrates were transferred into the vacuum for deposition of 10 nm MoO_3 and 100 nm Ag layers to complete the tandem device.

Device measurement

The I-V characteristic curve of PSC was recorded on the Keithley source unit under AM 1.5 G 1 sun intensity illumination by a solar simulator from Abet Corp. The intensity of the solar simulator is calibrated by a standard silicon diode, which was certified by National Renewable Energy Lab.

Results and discussion

Electrical properties of ZnO:Cs ETL

The work function of cathode or ETL is critical for device performance of OSCs. The lowered work functions are preferred to reduce the interfacial barriers for the electron extraction. UPS measurement is adopted to examine the work function variations of ZnO films with/without Cs_2CO_3 doping. As shown in **Figure 2a**, the pristine ZnO film shows a work function of 4.17 eV. However, with Cs_2CO_3 doping, the work function of ZnO:Cs film is lowered to 3.78 eV. **Figure 2b** shows

the energy level structures of all the layers in sequence of the device stacking. The work function 4.17 eV of the pristine ZnO film is higher than the LUMO of fullerene derivatives or the acceptors (3.9 eV for $PC_{61}BM$ or $PC_{71}BM$, and 3.74 eV for ICBA, **Figure 2b**), which indicates the possible formation of electron extraction barrier at the ITO cathode. However, the doped ZnO:Cs film shows a much lowered work function of 3.78 eV, which is comparable or even lower than the acceptor LUMO levels. As a result, the efficient electron injection from the ZnO:Cs layer to the acceptor is expected, which would induce electron Ohmic contact. In this regard, the ZnO:Cs film shows the promise for the further improving the device performance of OSCs.

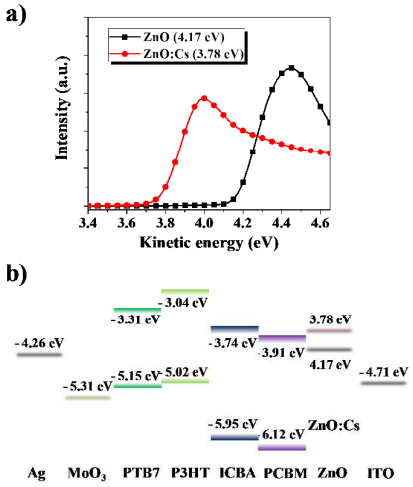

Figure 2. a） Ultra-Violet photoelectron spectroscopy of the pristine sol-gel ZnO and ZnO:Cs films. **b)** Energy level structure of each layer in the single junction organic solar cells.

The conductivity of the ZnO layer, especially along the vertical direction, is critical for efficient charge extraction and high device performance. Here, we investigated the vertical conductivity of ZnO:Cs films by the conducting mode AFM measurement. This technique allows to mapping the conductivity of each pixel on a small area and vertical to the films. The measurement of film conductivity is performed at contact mode, and a bias voltage of minus 2 V is applied. **Figure 3** shows the C-AFM images of 120 nm ZnO (**Figure 3a**) and ZnO:Cs films (**Figure 3b**) on the glass/ITO substrate. The current intensity of ZnO:Cs film is significantly stronger compared with that of the pristine ZnO film. This result clearly shows that the Cs_2CO_3 doping of sol-gel ZnO would increase the conductivity.

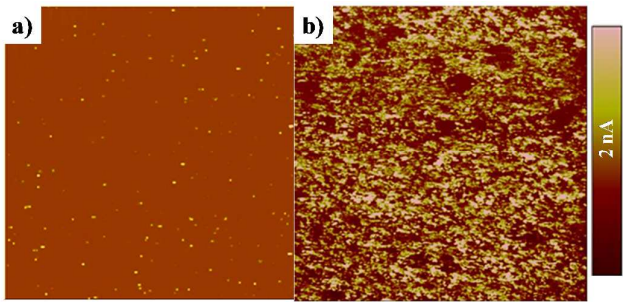

Figure 3. Conducting atomic force microscope images of **a)** the pristine ZnO (120 nm) and **b)** the doped ZnO:Cs (120 nm) films.

PV devices

To testify the efficacy of the doped Zn:Cs layer as ETL for photovoltaic devices, we fabricated solar cells based on a variety of photovoltaic materials systems, e.g. P3HT:$PC_{61}BM$, P3HT:ICBA, and PTB7:$PC_{71}BM$, in both single junction and tandem device architectures.

Organic single junction solar cells

The inverted single junction OSC device is used to evaluate the efficacy of the doped ZnO:Cs film as ELT. The device structure of ITO/ZnO or ZnO:Cs/active layer/MoO_3/Ag is presented in **Figure 1b**. The intensively studied organic photovoltaic materials, e.g. P3HT:$PC_{61}BM$, P3HT:ICBA, and PTB7:$PC_{71}BM$, were selected as the active layers to testify the versatility of ZnO:Cs as ETL. **Figure 4a** shows the I-V characteristics of these OSC devices, and the detailed device parameters are summarized in **Table 1**. As shown, the P3HT:$PC_{61}BM$ based single junction device with the pristine ZnO as ETL shows a J_{SC} of 8.61 mA/cm^2, a V_{OC} of 0.60 V, a FF of 0.628, and a power conversion efficiency (PCE) of 3.25%. With the doped ZnO:Cs layer as ETL, all the device parameters get increased, with a J_{SC} of 9.53 mA/cm^2, a V_{OC} of 0.62 V, a FF of 0.649, and a PCE of 3.84%. This constitutes a 18% enhancement in PCE compared with the control device. For the P3HT:ICBA based organic solar cell, the doping of sol-gel ZnO boosts the device PCE from 5.23% to 6.42%, J_{SC} from 10.32 to 11.41 mA/cm^2, and FF from 0.626 to 0.683. In the PTB7:$PC_{71}BM$ device, the device FF increases from 0.657 to 0.726, and device PCE increases from 7.01% to 7.89%. The enhancement in the J_{SC} of all of the single junction devices with the doped ZnO:Cs film could be confirmed by the EQE spectra shown in **Figure 4b** and **c**. As shown, for the P3HT based OSCs, the EQE spectra are enhanced in the whole absorption region. This indicates that the electron extraction at the cathode interface becomes more efficient, which could be attributed to the improved Ohmic contact at the cathode interface. However, for the PTB7:$PC_{71}BM$ system, the EQE is only slightly enhanced in the $PC_{71}BM$ absorption region, consistent to the slight increase of J_{SC} (from 14.42 to 14.88 mA/cm^2). This could be attributed to the suppression exciton quenching in PCBM phase, which is possibly resulted from the faster charge transfer at the interface of ZnO:Cs/$PC_{71}BM$.

The general enhancement of device performance based on a variety of popular device system with the doped ZnO:Cs suggests the efficacy and versatility of the ZnO:Cs as an efficient ETL in OSC. We attribute the decent device performance enhancement to the lowered work function and the increased charge transporting with Cs doping, which could be derived from the decreased series resistance (R_s) of the OSC devices based on all the three materials systems upon doping (**Table 1**).

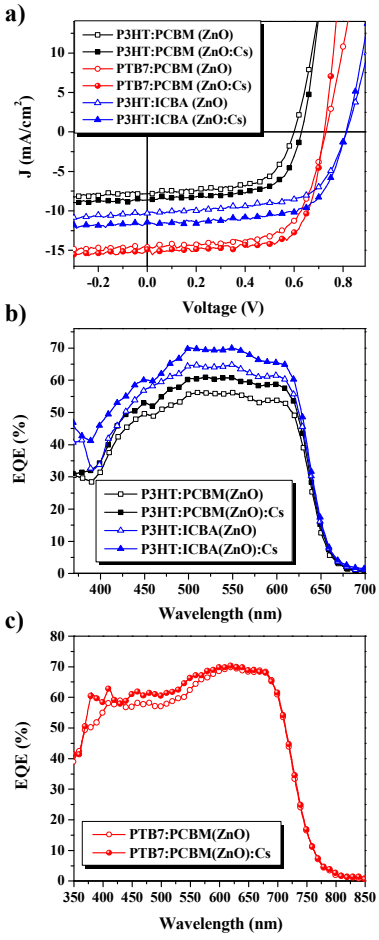

Figure 4. **a)** I-V characteristics of P3HT:$PC_{61}BM$, PTB7:$PC_{71}BM$, and P3HT:ICBA based OSCs with ZnO and ZnO:Cs as ETL. **b)** EQE spectra of P3HT based solar cells (P3HT:$PC_{61}BM$ and P3HT:ICBA) with ZnO and ZnO:Cs as ETL, **c)** EQE spectra of PTB7:$PC_{71}BM$ based solar cells with ZnO and ZnO:Cs as ETL.

Table 1. Device parameters of P3HT:$PC_{61}BM$, PTB7:$PC_{71}BM$, and P3HT:ICBA based single junction and tandem photovoltaic devices with ZnO and ZnO:Cs as ETLs

Active layer	ETL	J_{SC} (mA/cm^2)	V_{OC} (V)	FF (/)	Efficiency (%)		R_s (Ω/cm^2)
					Best	Ave.	
P3HT:$PC_{61}BM$	ZnO	8.61	0.60	0.63	3.25	3.14±0.03	5.2
	ZnO:Cs	9.53	0.62	0.65	3.84	3.59±0.06	3.4
P3HT:$C_{60}BA$	ZnO	10.32	0.81	0.63	5.23	5.02±0.08	7.2
	ZnO:Cs	11.41	0.81	0.68	6.42	5.89±0.18	4.1
PTB7:$C_{71}BM$	ZnO	14.42	0.73	0.67	7.01	6.84±0.05	1.4
	ZnO:Cs	14.88	0.73	0.73	7.89	7.59±0.11	1.2
Tandem	ZnO	8.14	1.53	0.64	8.03	7.71±0.11	7.7
	ZnO:Cs	8.16	1.52	0.69	8.56	8.02±0.21	4.3

ZnO:Cs thickness dependent device performance

As mentioned, the interfacial layer design with OSC device performance insensitive to the layer thickness is required to be robust for device manufacturing. In this regard, interfacial layer with high conductivity is favored. One of the most prominent features with the doped ZnO:Cs film is the decent increase in conductivity, as revealed by the C-AFM measurement. Here, we fabricated OSC devices with different thicknesses of ETL to examine the efficacy of ZnO:Cs as the robust ETL. The PTB7:$PC_{71}BM$ blend is used as the active layer in the devices. **Figure 5** shows the I-V characteristics of the devices with different thicknesses of ZnO:Cs as ELT. For comparison, the OSC devices with different thicknesses of the pristine sol-gel ZnO layer as ETL are also fabricated, with their I-V characteristics shown in **Figure 5a**. Due to the optical spacer effect, the J_{SC} of organic solar cells would vary with the thickness of ZnO layer [28]. Also, the thicker ZnO or ZnO:Cs film would induce the severe edge effect due to the increased conductance[43], which resulting in the overestimation of J_{SC}. Therefore, the origin of J_{SC} variation with different thicknesses of ZnO or ZnO:Cs film is confusing. It is very difficult to distinguish the doping effect, the optical spacer or the edge effect counting for the variation of J_{SC}. Besides of the J_{SC}, the FF is also influenced by and even more sensitive to the interfacial contact at the cathode. Here, we normalized the J_{SC} for each I-V curve and observed the FF variation with the thickness of ZnO or ZnO:Cs ETL. The variations of FF with the ETL thickness of ZnO or ZnO:Cs are shown in **Figure 5c**. For OSCs with the pristine ZnO as ETL, the FF drops dramatically with the ZnO thickness beyond 80 nm, which is corresponding to the concave of I-V curve with increasing the ZnO thickness. Accordingly, the R_s of OSC increases from 1.41 to 4.97 Ω/cm^2, and R_{sh} dramatically decreases from 1.21×10^5 to 1.79×10^3 Ω/cm^2 with increasing the ZnO thickness. In the case of the doped ZnO:Cs, the FF increases (0.74) with the thickness coming to 80 nm. Further increase in the ZnO:Cs thickness shows little influence on the FF of the device, where the FF of the device remains 0.67 even the thickness of the ZnO:Cs

comes to 520 nm. Correspondingly, the R_s varies from 1.21 to 2.56 Ω/cm^2 and R_{sh} from 8.72×10^5 to 9.37×10^4 Ω/cm^2 with the thickness of ZnO:Cs increasing from 40 to 520 nm. **Figure 5d** shows the I-V characteristics of OSC with 320 nm ZnO or ZnO:Cs as ETL at dark, which directly shows the leakage current is significantly suppressed and forward current enhanced with the doped ZnO:Cs ETL. The insensitivity of the device FF with the thickness of ZnO:Cs indicates the robustness of ZnO:Cs as ETL for application in OSC. These results verify the potential of the doped Zn:Cs film as an efficient and robust ETL for developing highly efficient printable OSCs.

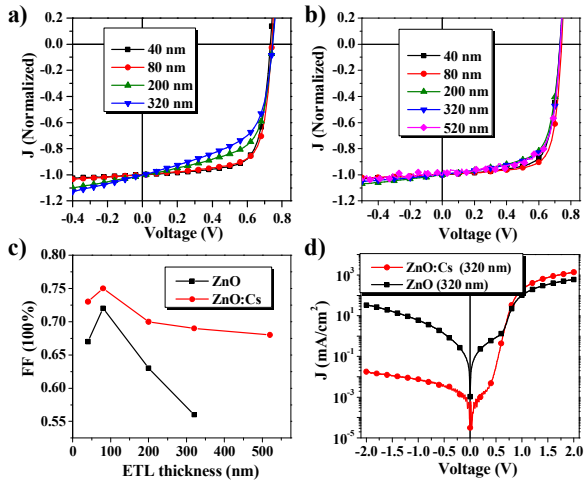

Figure 5. I-V characteristics of PTB7:PC_{71}BM solar cells with different thicknesses of the pristine ZnO (**a)** and the doped ZnO:Cs (**b)** as ETL. **c)** Variation of FF with the thickness of the pristine ZnO and the doped ZnO:Cs ETLs. **d)** Dark I-V characteristics of PTB7:PC_{71}BM solar cells with 320 nm thickness of the pristine ZnO or the doped ZnO:Cs as ETL.

Table 2. Device parameters of PTB7:PC_{71}BM based single junction photovoltaic devices with different thicknesses of the pristine ZnO and the doped ZnO:Cs as ETLs.

ETL	Thickness nm	FF /	Rs Ω/cm^2	Rsh Ω/cm^2
ZnO	40	0.67	1.41	1.21×10^5
	80	0.72	1.11	7.09×10^4
	200	0.63	3.52	1.26×10^4
	320	0.56	4.97	1.79×10^3
ZnO:Cs	40	0.73	1.21	8.72×10^5
	80	0.75	0.97	1.12×10^6
	200	0.70	1.98	2.58×10^5
	320	0.69	2.32	3.46×10^5
	520	0.68	2.56	9.37×10^4

Organic tandem solar cells

Series connected tandem architecture has the potential to efficiently utilize the solar irradiance for OSCs, in which the ETL is also very important for high device performance. Here, series connected tandem device architecture (**Figure 1c**) is designed to test the efficacy of the ZnO:Cs as ETL. We used the P3HT:ICBA blend as the front cell active layer due to the large band gap (~2.0 eV) of P3HT and the high V_{OC} for the thermalization loss reduction, and PTB7:PC_{71}BM blend as the back cell active layer due to the low band gap (~ 1.7 eV) and the potential for transmittance loss alleviation. The UV-Visible absorption spectra of P3HT:ICBA and PTB7:PC_{71}BM films are shown in **Figure 6a**. The complementary absorption spectra indicates the suitability of the two systems to compose a series tandem device, where the current density of sub-cells should be matched. The interconnecting layer composed of the modified PEDOT:PSS and ZnO/ poly[(9,9-bis(3-(N,N-dimethylamino)-propyl)-2,7-fluorene)-alt-2,7-(9,9-dioctylflorene)] (PFN) multi-layers for the sub-cells connection. The doped ZnO:Cs and MoO_3 were used as ETL and HTL, respectively. The I-V curves of the tandem devices with the pristine ZnO and the doped ZnO:Cs as ETLs are shown in **Figure 6b**. After optimization, the best device performance of the tandem solar cells with the doped ZnO:Cs as ETL shows a PCE of 8.56%, a V_{OC} of 1.53 V, an FF of 0.69, and a J_{SC} of 8.16 mA/cm^2, which exhibits appreciable enhancement compared to that with the pristine ZnO as ETL. With regard to each individual cell, the PCE of the tandem solar cell is also improved (see **Table 1**). The V_{OC} of the tandem solar cell is nearly the summed value of the two sub-cells. Especially, the FF of the tandem device is approaching 70%. These results indicate the efficacy of the doped ZnO:Cs layer as ETL in series connected tandem organic solar cells.

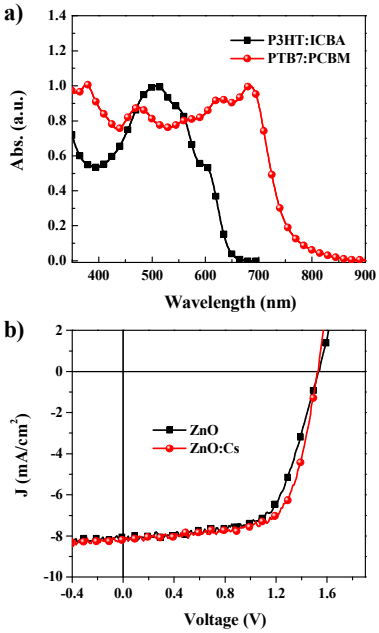

Figure 6. a) UV-Visible absorption spectra of P3HT:IC_{60}BA and PTB7:PC_{71}BM films. **b)** I-V characteristics of organic tandem solar cells with the pristine ZnO or the doped ZnO:Cs as ETL. The tandem device structure: glass/ITO/ZnO or ZnO:Cs/ P3HT:ICBA/PEDOT:PSS/ZnO/PFN/PTB7:PC_{71}BM/MoO_3/Ag.

Conclusion

In summary, we demonstrate the Cs_2CO_3 doped sol-gel ZnO is an efficient and robust ETL with versatile application for a wide range of organic solar cells, e.g. P3HT:PC_{61}BM, P3HT:ICBA, and PTB7:PC_{71}BM in both single junction and tandem device structures. With the Cs_2CO_3 doping, the work function of the sol-gel ZnO is lowered, and the conductivity is increased significantly, which reduces the extraction barrier. Remarkably, the device performance shows marginal drop with the thickness of the doped ZnO:Cs ETL ranging from 40 to 520 nm, indicating its robustness for roll to roll integration. We stress the importance of chemical doping method for developing highly efficient interfacial layer, and the potential of the doped ZnO:Cs film as efficient and robust ETL for device optimization and future commercialization.

Acknowledgements

This work was supported by the Major State Basic Research Development Program (2014CB643503), the National Natural Science Foundation of China (Grants 91233114 and 51261130582), the Postdoctoral Science Foundation of China (2015M570505), and the program for Innovative Research Team in University of Ministry of Education of China (IRT13R54).

References

1 J. Peet, M. L. Senatore, A. J. Heeger and G. C. Bazan, *Adv. Mater.*, 2009, **21**, 1521-1527.
2 B. C. Thompson and J. M. J. Fréchet, *Ang. Chem. Int. Edit.*, 2008, **47**, 58-77.
3 M. Gratzel, *Nat. Mater.*, 2014, **13**, 838-842.
4 T. D. Nielsen, C. Cruickshank, S. Foged, J. Thorsen and F. C. Krebs, *Sol. Energ. Mater. Sol. C.*, 2010, **94**, 1553-1571.
5 H. Spanggaard and F. C. Krebs, *Sol. Energ. Mater. Sol. C.*, 2004, **83**, 125-146.
6 F. C. Krebs, *Sol. Energ. Mater. Sol. C.*, 2009, **93**, 465-475.
7 F. C. Krebs, T. Tromholt and M. Jorgensen, *Nanoscale*, 2010, **2**, 873-886.
8 Z. He, C. Zhong, S. Su, M. Xu, H. Wu and Y. Cao, *Nat. Photon.*, 2012, **6**, 591-595.
9 J. You, L. Dou, K. Yoshimura, T. Kato, K. Ohya, T. Moriarty, K. Emery, C.-C. Chen, J. Gao, G. Li and Y. Yang, *Nat. Commun.*, 2013, **4**, 1446.
10 L.-J. Zuo, X.-L. Hu, T. Ye, T. R. Andersen, H.-Y. Li, M.-M. Shi, M. Xu, J. Ling, Q. Zheng, J.-T. Xu, E. Bundgaard, F. C. Krebs and H.-Z. Chen, *J. Phys. Chem. C*, 2012, **116**, 16893-16900.
11 Y. Hirose, A. Kahn, V. Aristov, P. Soukiassian, V. Bulovic and S. R. Forrest, *Phys. Rev. B*, 1996, **54**, 13748-13758.
12 S. R. Cowan, P. Schulz, A. J. Giordano, A. Garcia, B. A. MacLeod, S. R. Marder, A. Kahn, D. S. Ginley, E. L. Ratcliff and D. C. Olson, *Adv. Funct. Mater.*, 2014, **24**, 4671-4680.
13 R. A. Street, M. Schoendorf, A. Roy and J. H. Lee, *Phys. Rev. B*, 2010, **81**, 205307.
14 14.Z.-K. Tan, K. Johnson, Y. Vaynzof, A. A. Bakulin, L.-L. Chua, P. K. H. Ho and R. H. Friend, *Adv. Mater.*, 2013, **25**, 4131-4138.
15 L. Zuo, J. Yao, H. Li and H. Chen, *Sol. Energ. Mater. Sol. C.*, 2014, **122**, 88-93.
16 W. Tress, K. Leo and M. Riede, *Adv. Funct. Mater.*, 2011, **21**, 2140-2149.
17 R. Po, C. Carbonera, A. Bernardi and N. Camaioni, *Energ. Environ. Sci.*, 2011, **4**, 285-310.
18 R. Steim, F. R. Kogler and C. J. Brabec, *J. Mater. Chem.*, 2010, **20**, 2499-2512.
19 E. D. Gomez and Y.-L. Loo, *J. Mater. Chem.*, 2010, **20**, 6604-6611.
20 L.-M. Chen, Z. Xu, Z. Hong and Y. Yang, *J. Mater. Chem.*, 2010, **20**, 2575-2598.
21 E. L. Ratcliff, B. Zacher and N. R. Armstrong, *J. Phys. Chem. Lett.*, 2011, **2**, 1337-1350.
22 J. Huang, P. F. Miller, J. S. Wilson, A. J. de Mello, J. C. de Mello and D. D. C. Bradley, *Adv. Funct. Mater.*, 2005, **15**, 290-296.
23 H. Gommans, B. Verreet, B. P. Rand, R. Muller, J. Poortmans, P. Heremans and J. Genoe, *Adv. Funct. Mater.*, 2008, **18**, 3686-3691.
24 P. Peumans and S. R. Forrest, *Appl. Phys. Lett.*, 2001, **79**, 126-128.
25 M. F. Lo, T. W. Ng, S. L. Lai, F. L. Wong, M. K. Fung, S. T. Lee and C. S. Lee, *Appl. Phys. Lett.*, 2010, **97**, -.
26 C. J. Brabec, S. E. Shaheen, C. Winder, N. S. Sariciftci and P. Denk, *Appl. Phys. Lett.*, 2002, **80**, 1288-1290.
27 Y. Sun, J. H. Seo, C. J. Takacs, J. Seifter and A. J. Heeger, *Adv. Mater.*, 2011, **23**, 1679-1683.
28 S. H. Park, A. Roy, S. Beaupre, S. Cho, N. Coates, J. S. Moon, D. Moses, M. Leclerc, K. Lee and A. J. Heeger, *Nat. Photon.*, 2009, **3**, 297-302.
29 Y. Gao, H.-L. Yip, K.-S. Chen, K. M. O'Malley, O. Acton, Y. Sun, G. Ting, H. Chen and A. K. Y. Jen, *Adv. Mater.*, 2011, **23**, 1903-1908.
30 G. Parthasarathy, C. Shen, A. Kahn and S. R. Forrest, *J. Appl. Phys.*, 2001, **89**, 4986-4992.
31 M. Rusu, S. Wiesner, I. Lauermann, C.-H. Fischer, K. Fostiropoulos, J. N. Audinot, Y. Fleming and M. C. Lux-Steiner, *Appl. Phys. Lett.*, 2010, **97**, -.
32 L. Motiei, Y. Yao, J. Choudhury, H. Yan, T. J. Marks, M. E. v. d. Boom and A. Facchetti, *J. Am. Chem. Soc.*, 2010, **132**, 12528-12530.
33 L. Zuo, X. Jiang, M. Xu, L. Yang, Y. Nan, Q. Yan and H. Chen, *Sol. Energ. Mater. Sol. C.*, 2011, **95**, 2664-2669.
34 Y. Zhou, C. Fuentes-Hernandez, J. Shim, J. Meyer, A. J. Giordano, H. Li, P. Winget, T. Papadopoulos, H. Cheun, J. Kim, M. Fenoll, A. Dindar, W. Haske, E. Najafabadi, T. M. Khan, H. Sojoudi, S. Barlow, S. Graham, J.-L. Brédas, S. R. Marder, A. Kahn and B. Kippelen, *Science*, 2012, **336**, 327-332.
35 H. Wang, E. D. Gomez, Z. Guan, C. Jaye, M. F. Toney, D. A. Fischer, A. Kahn and Y.-L. Loo, *J. Phys. Chem. C*, 2013, **117**, 20474-20484.
36 R. Søndergaard, M. Hösel, D. Angmo, T. T. Larsen-Olsen and F. C. Krebs, *Mater. Today*, 2012, **15**, 36-49.
37 F. C. Krebs, R. Søndergaard and M. Jørgensen, *Sol. Energ. Mater. Sol. C.*, 2011, **95**, 1348-1353.
38 D. Gao, M. G. Helander, Z.-B. Wang, D. P. Puzzo, M. T. Greiner and Z.-H. Lu, *Adv. Mater.*, 2010, **22**, 5404-5408.
39 Z. Lu, J. Zhou, A. Wang, N. Wang and X. Yang, *J. Mater. Chem.*, 2011, **21**, 4161-4167.
40 S. Kwon, K.-G. Lim, M. Shim, H. C. Moon, J. Park, G. Jeon, J. Shin, K. Cho, T.-W. Lee and J. K. Kim, *J Mater. Chem. A*, 2013, **1**, 11802-11808.
41 Z. Zulkifli, M. Subramanian, T. Tsuchiya, M. S. Rosmi, P. Ghosh, G. Kalita and M. Tanemura, *RSC Advances*, 2014, **4**, 64763-64770.
42 Z. Zulkifli, G. Kalita and M. Tanemura, *physica status solidi (RRL) – Rapid Research Letters*, 2015, **9**, 145-148.

43 D. Gupta, M. Bag and K. S. Narayan, *Appl. Phys. Lett.*, 2008, **93**, 163301.
44 L. Zuo, C.-C. Chueh, Y.-X. Xu, K.-S. Chen, Y. Zang, C.-Z. Li, H. Chen and A. K. Y. Jen, *Adv. Mater.*, 2014, **26**, 6778-6784.

Versatility and robustness of ZnO:Cs electron transporting layer for printable organic solar cells

Lijian Zuo, Shuhua Zhang, Shuai Dai, Hongzheng Chen*

State Key Laboratory of Silicon Materials, MOE Key Laboratory of Macromolecular Synthesis and Functionalization, Department of Polymer Science & Engineering, Zhejiang University, Hangzhou 310027, China, E-mail: hzchen@zju.edu.cn

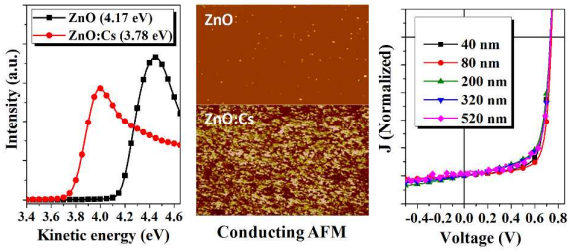

The Cs doped ZnO:Cs exhibits higher conductivity and lowered work function, and improves the device performance, which shows insensitive to the ZnO:Cs thickness.